Civil Engineering Infrastructures Journal xx,xx
DOI: 10.22059/CEIJ.2024.368614.1987

Behavior of Sheet Pile Wall Adjacent to a Square and Circular Footing

Abhijit Debnath[1] and Sujit Kumar Pal[2*]

[1] Ph.D. Candidate, Department of Civil Engineering, National Institute of Technology Agartala, Tripura 799046, India.

E-mail: abhijit.nita2020@gmail.com

Orcid ID: https://orcid.org/0000-0001-9665-7928

[2] Professor, Department of Civil Engineering, National Institute of Technology Agartala, Tripura 799046, India.

[*] Corresponding author E-mail: skpal1963@gmail.com

Orcid ID: https://orcid.org/0000-0003-2335-4680

Received: 25/11/2023
Revised: 16/03/2024
Accepted: 24/04/2024

ABSTRACT:

Deep excavations are frequently carried out near structural foundations in densely populated metropolitan areas. Those foundations surrounding the excavation site can impose additional lateral pressure on the retaining wall along with backfill pressure. A three-dimensional finite element analysis has been performed in the present study to determine the effect of square and circular footings of the same plan area on the sheet pile wall behavior. A parametric study is performed by varying the plan area of footing, embedded depth of sheet pile, magnitude of

surcharge loads, position of footing above and below the backfill surface from the top edge of the wall, the depth of the loose soil layer, and dredge line slope angle to find out the wall deflection, bending moment, and backfill ground settlement. The results show that the effect of square and circular footing highly influences the wall and backfill soil. However, the effect of square footing on the wall and backfill soil is more substantial than that of circular footing for the same plan area.

Keywords: Sheet Pile, Finite Element Analysis, Square Footing, Circular Footing, Dredge Line Slope Angle.

1. Introduction

Cantilever sheet pile walls (CSPW) are often recommended for shallow excavation depths (normally less than 5 m) since their stability is primarily dependent on the development of passive resistance below the dredge level (Fall et al., 2019; Singh and Chatterjee, 2020a). The existence of surcharge load in the form of the building foundation, vehicle, and other permanent structures on the backfill soil produces additional stress on the wall, thus triggering higher wall deflection, bending moment (BM), and ground settlement (GS) (Singh and Chatterjee, 2020b). Several studies have been performed on sheet pile wall (SPW) numerically, experimentally, and analytically for many years. Sowers and Sowers (1967) discuss various cases of failures of anchored bulkhead. They found that anchored SPW failures were governed by excessive lateral earth pressures (EPs), lack of attention to deflection, and the influence of construction techniques. In the sand, experiments are carried out out to investigate how sloping dredge lines affect the foreslope passive resistance and sheet pile BMs (Schroeder and Roumillac, 1983). Bose and Som (1998) used the finite element (FE) method to examine the excavation behavior of the diaphragm wall in the Calcutta Metro under the sequential excavation process and strut installation. Georgiadis and Anagnostopoulos (1998) did an experimental study in the sand

with surcharge strip loads. Model test results are compared to BMs calculated using several lateral EP theories and with the results of the FE study by PLAXIS. The computer program FLAC has been used to develop a FE model for a braced excavation to estimate the different design parameters that has a significant impact on excavation behavior (Chowdhury et al., 2013). The impacts of the penetration depth have been studied to evaluate the diaphragm wall behavior during excavations in sand by the 3D numerical analysis (Bahrami et al., 2018). Ahmadpour et al. (2018) considered a sheet pile supporting excavation system to study the effects of the loose soil layer on deflection and SPWs lateral supporting systems using PLAXIS 2D FE software. A case study and numerical simulation were conducted on a foundation pit that was supported by U-shaped SPW (Wang et al., 2019). Basha and Elsiragy (2019) conducted a numerical study to examine how SPW driving affects the geotechnical behavior of nearby buildings in the sand. An experimental investigation has been executed to know the SPW behavior nearby to a pre-existing footing (Aparna and Samadhiya, 2019). Singh and Chatterjee (2020c) investigate the impact of distance between the uniform surcharge and CSPW of varying embedded depths to determine the BM, horizontal EP, deflection, and settlement by FLAC2D. A finite element analysis was performed to investigate the forces in the strut and the estimated earth pressures for braced excavations in anisotropic clay under a plane strain condition (Zhang et al., 2021). Three-dimensional numerical modeling has been performed by ABAQUS to evaluate the behavior of a deep excavation supported by a tie-back wall (Tabaroei et al., 2022). Laboratory tests and numerical analyses were performed by PLAXIS 3D software to determine SPW deformation and bearing capacity of the foundation with vertical loads applied by a model foundation (Ozpolat and Aksoy, 2022). Pradeep et al. (2022) used hybrid ANN with optimization techniques to access the reliability of embedded depth of CSPWs, with cohesive soil below dredge level and cohesionless backfill soil. Li et al. (2022) did a numerical analysis of clay soil on the performance of braced excavation,

considering the soil's stress-induced anisotropic behavior. A three-dimensional FE study has been performed to identify the effect of strip load as surcharge on the anchored SPW deflection, BM, anchor forces and settlement of the backfill ground surface (BGS) (Debnath and Pal, 2023a). PLAXIS 3D FE software will be utilized to analyze the impact of nearby deep excavation on the performance of a loaded individual pile in sandy soil (Hakeem, 2024).

The available literature shows that no attention has been given to the effect of the footing positioned at different depths below the backfill surface on the behavior of sheet pile. No literature exists to analyze the shape effect of footing on the sheet pile behavior. Furthermore, very few articles concentrate on the impact of sloping dredge lines on the behavior of SPW. Hence, a numerical analysis with realistic 3D modeling by ABAQUS FE-based software has been performed to bridge the existing research gap, emphasizing the shape effect of footings (circular and square) positioned at different locations above and below the BGS. A parametric study was implemented to find the impact of various parameters effecting the deflection, BM, and backfill GS. The laboratory experiments have been done to validate the present numerical model.

2. Numerical Modeling

2.1. Soil and Wall Profiles

A three-dimensional FE analysis was used to model the soil and wall. Dense sand is used for the entire FE analysis and loose sand is employed in layers to replace dense sand from the BGS in order to study the impact of loose soil layers on the SPW behavior. The soil properties are adopted from Singh and Chatterjee (2020a, c), presented in Table 1. The PZ27 sheet pile is adopted from the USS sheet piling design manual (Manual, 1984), as selected by Bilgin (2012). The properties of the sheet pile section are presented in Table 2. The overall wall height is taken as 11.00 m with an excavated depth (H) of 4.50 m and an embedded depth (D) of 6.50

m. The hydrostatic forces balance each other when the water level elevation is equal on either side of the wall (Bilgin, 2012). Hence, in the current study, the elevation of the water table is assumed at 2 m depth on either side of the wall from the wall top edge during the complete analysis. Therefore, the soil is considered to be completely saturated under the water table.

[Insert Table 1]

[Insert Table 2]

2.2. Finite Element Analysis

ABAQUS FE code has been used for the 3D modeling of SPW, footing, and soil. The soil has been modeled using the Mohr-Coulomb model with a non-associated flow rule as several researchers have successfully used it to model the cohesionless soils of retaining walls (Hsiung, 2009; Bilgin, 2012; Chowdhury et al., 2013; Bahrami et al., 2018; Ahmadpour et al., 2018; Fall et al., 2019; Guo et al., 2019; Singh and Chatterjee, 2020a, c; Debnath and Pal, 2023b). The SPW and the footings are modeled as linear elastic materials. The current study chooses the soil-SPW and soil-footing contact to impose the interaction properties. Different options for defining the contact zone are available in ABAQUS, including “node-to-surface” and “surface-to-surface”. The “surface-to-surface” contact is applied in this study due to its accuracy. According to the master-slave concept, the master surface is the harder surface and the master surface is permitted to penetrate into the slave surface (ABAQUS, 2012). The sheet pile and footings are selected as the master surface when considering the interaction between soil-SPW and soil-footing, while the soil mass is treated as the slave surface. During the construction in the field no walls are constructed perfectly smooth; hence, to include the roughness effect of the wall, the interface friction angle is adopted as 2/3 times the soil friction angle (Bahrami et al., 2018; Singh and Chatterjee, 2020a, c). To obtain a higher degree of accuracy and efficient simulations with less effort sensitivity analysis and mesh refinement is

performed. The soil mass, sheet pile and footings are modeled by a 20-nodded hexahedral quadratic brick element with reduced integration (C3D20R). In order to diminish the impact of boundary conditions on the numerical findings, the numerical model boundaries must be kept sufficiently large. Singh and Chatterjee (2020a, b) adopted numerical model boundaries are used in the present investigation. Hence, in the present study, the depth of the numerical model boundary below the base of the sheet pile was assumed to be five times the overall wall height and the length of the model was selected as sixteen times the overall wall height (eight times both behind and in front of the wall) for the cases analyzed in this study because increasing the overall depth and length of the model boundary beyond these dimensions does not effect the numerical analysis results. The numerical model width was kept five times the width of the square footing ($5 \times 2.50 = 12.50$ m). According to Singh and Chatterjee (2020a, b), the selected dimensions are adequate and safe compared to Chowdhury et al. (2013). Figure 1 shows the dimensions, element type, model meshing and model boundaries adopted for the numerical study. The SPW is placed in the middle of the model width. According to the construction sequence, sheet piles are classified as backfilled construction and dredging construction (Tsinker, 1983). The present study implements the dredging structure during numerical modeling and analysis. The sequences of dredging construction are sheet pile driving, backfilling (if necessary), and dredging of frontfill soil.

The numerical modeling has been made in the following steps: at the initial step to obtain equilibrium condition geostatic stress is imposed in the model, before the sheet pile installation and lateral EP co-efficient at rest (K_0) has been applied and estimated by Jaky's equation (Jaky, 1944), which is $(1 - \sin \phi)$; where ϕ is the friction angle of soil. Later on the SPW is introduced in the soil continuum and the self-weight is induced into the whole model to reach the model to an equilibrium position again. After that, the vertical surcharge load of different magnitudes is imposed by a model footing. Finally, the frontfill soil excavation starts

sequentially by soil lifting in four steps, the thickness of each lift is 1.125 m, to include the influence of construction techniques throughout the analysis. As the loads are imposed quickly, so, the influence of consolidation and pore pressure changes does not consider during the FE analysis (Deb and Pal, 2019).

[Insert Fig. 1]

3. Experimental Study

To study the sheet pile wall behavior, a small-scale laboratory experiment was executed. The model test set-up and experimentation were carried out in three stages: Stage 1 involved soil bed preparation and sheet pile installation, Stage 2 involved the application of vertical load, and in Stage 3 the sequential excavation of frontfill soil was done. The test set-up and the stages of experimentation are illustrated in Figure 2. The model SPW and footing specifications have been chosen according to the scaling laws (Wood, 2004) as shown in Table 3. The laboratory model dimensions have been chosen with a scaling ratio of n (model/prototype) is equal to 30 in order to simulate the small-scale experimental model with the prototype numerical model. The plan area of the model footing is taken as 69.44 cm^2 (6.25 m^2) (The equivalent prototype area is 62500 cm^2). The experimental set-up consists of a testing tank, where the depth of the tank below the dredge line is selected as five times the height of the SPW above the dredge level (5H) and the backfill length is six times the height of the SPW above the dredge level (6H) in order to retain the developed soil stress inside the tank boundary. Hence, the overall dimensions of the tank are 1.80 m × 0.90 m (length × depth) and the width is kept at 0.75 m. The test tank is made up of a 10 mm thick translucent Perspex-sheet on the vertical sides and a steel sheet 10 mm thick in the base. Adding a Perspex-sheet on all vertical sides of the testing tank reduces friction between the tank and soil particles. While preparing the dense soil bed, a uniform density is maintained throughout the testing chamber using controlled pouring and

tamping procedures. In this procedure, the amount of sand required for each layer to produce a particular relative density was first weighted, then deposited in the tank and tamped until the required layer height was achieved. To ensure a consistent relative density throughout the sand bed, four cylindrical Aluminum containers are placed at various positions. During the preparation of the sand bed, a tolerance in relative density of 1.50% to 2.10% is accepted. The soil is poured upto the base of the SPW during the first step of soil bed preparation. The model SPW is then placed in the centre of the test chamber and held in place with detachable temporary supports, ensuring the verticality of the sheet pile throughout the soil bed preparation. After that, the soil is again poured upto the top of the wall and the temporary supports are removed before the beginning of experimentation. A steel frame is used as a loading frame; a 20 ton capacity hydraulic system is used for applying the vertical load; a 30 kN capacity load cell having an accuracy of 0.01 kN is used to measure the amount of vertical load; linear variable displacement transducers (LVDTs) with a sensitivity of 0.01 mm are utilized for measuring the lateral wall deflection; a data acquisition system connected with computer to record data directly during the experimentation. The applied load with the hydraulic jack is first transferred to the cylindrical shaft and subsequently to the foundation via the load cell as presented in Figure 2. The load cell is compressed during loading and records the applied vertical load. During the entire experimentation program, constant surcharge pressure is maintained and lateral deflection of the SPW is recorded after the end of the fourth excavation stage. The experimentation has been done in this study only for validation.

[Insert Fig. 2]

[Insert Table 3]

4. Validation of the Numerical Model

The developed numerical model is validated with experimental test results to ensure higher

accuracy in numerical studies. A similar soil profile and model boundary conditions are maintained while performing experimental analysis to compare the results obtained from the experiment with the numerical results. The experimentation has been done by performing tests with square and circular footing with a 100 kPa surcharge load positioned at the wall top edge. Figure 3a and 3b show the comparison of wall deflection results for square and circular footing respectively, with equal plan area in dense sand. The figure shows that the deflection profile achieved from the numerical model study and the laboratory model test show a similar trend. Figure 3a illustrates that the maximum wall deflection is 63.00 mm for the proposed FE model compared to 54.50 mm found in the experimental study for a square footing. Similarly, Figure 3b illustrates that the maximum wall deflection is 51.00 mm for the proposed FE model for circular footing compared to 43.00 mm found in the experimental study. The results of the two studies shows a small difference in the deflection results, which could be due to the different approaches to analysis. Hence, the proposed numerical model test results are very close to the experimental results, thus the numerical model and experimental work agreed well.

[Insert Fig. 3]

[Insert Table 4]

5. Results and Discussions

A numerical analysis by the FE method has been executed, emphasizing the shape effect of footings positioned at different locations to investigate the behavior of SPW. To determine wall deflections, BMs, and backfill GS, a parametric study is conducted by changing various parameters such as the magnitude of the surcharge load, plan area of footing, wall penetration depth, square and circular footing position along the BGS and depth of the wall, depth of loose soil layer, and dredge line slope inclination. More explanations regarding each parameter are described in detail in the following subsections. The description of the different parametric

data used is described in Table 4. All the analysis has been performed in the dense sand, except the study of the effect of loose layer on SPW and backfill GS.

5.1. Effect of Varying Plan Area of Square and Circular Footing on Maximum Wall Deflection and Bending Moment

The effect of varying plan area of square and circular footing on maximum wall deflection and BM are determined by placing the footing at the wall top edge (X = 0.000 m, Y = 0.000 m) with a 75 kPa surcharge. Figure 4a and 4b illustrates the maximum deflection and BM respectively, for varying plan area of the footing. The maximum deflection and BM increase as the plan area of the square and circular footings increases. The increment is less upto a footing area of 4.00 m^2; after that, it is found to be significantly increased and reaches its maximum value at a footing area of 12.25 m^2 as shown in Figure 4a and 4b. The reason is that the higher footing area displaces a higher amount of backfill soil below it, producing higher lateral pressure to the wall, leading to a higher deflection and BM. Figures show that the square footing has a substantially greater impact on wall deflection and BM than a circular footing of the same plan area. For example, a plan area of footing 6.25 m^2 produces 1.22 and 1.68 times higher wall deflection and BM respectively, than a circular footing under 75 kPa surcharge load for dense sand. This is because the shape effect of square and circular footing (Shafiqul Islam et al., 2017). The horizontal displacement contours of soil for circular footings were developed around the edge of the footing and transmitted to the outward direction of the footing; the extent of the contours was uniform and circular, similar to the footing area. However, due to the corner effect of square footings, the horizontal displacement contours of the square footing were produced first at the corners and then moved to the footing edges. These contours are finally travelled in the outward direction of the footing area. The extent of the contours was found to be maximum at the centre point of the footing edges and minimum

at the corner regions of the footing. Because of the higher lateral deformation produced at the middle of the square footing edge due to the corner effect compared to circular footing, hence, the square footing influences the SPW behavior more than circular footing. In the present study, an equal footing area of 6.25 m^2 for both square and circular-shaped footing has been adopted for the complete analysis.

[Insert Fig. 4]

5.2. Influence of Embedded Depth on Maximum Wall Deflection and Bending Moment

Various trial embedded depths are chosen to understand the behavior of the wall with square footing positioned at the walls top edge. The present study analyzes 4.50, 6.50, 8.50, and 10.50 m embedded depths. Figure 5a and 5b show the profile of maximum wall deflection and BM respectively, with different surcharge loads. It has been found that the shallow embedded depth of the wall highly influences the deflection and BM, due to the full mobilization of passive earth resistance (occurs upto plastic zone below the dredge level), which takes place at a larger depth for shallow embedded depth wall below the dredge level. But beyond 6.50 m, the influence of embedded depth on maximum deflection and BM significantly reduces because, at the higher embedded depths the wall deflection and BM significantly reduce because of the development of a plastic zone below the dredge level and net EP at the base of the wall decreases. This decrease in the extension of the plastic zone below the dredge level and the net EP at the base of the wall can be attributed to a significant decrease in the horizontal wall movement. The observed trends are consistent with the findings of Singh and Chatterjee (2020a). For example, a reduction in maximum wall deflection of 0.79, 0.74, and 0.73 times is observed for embedded depths of 6.50, 8.50, and 10.50 m respectively, than 4.50 m embedded depth for 150 kPa surcharge load. Similarly, an increase in maximum BM of 1.41, 1.54, and

1.62 times is observed for embedded depths of 6.50, 8.50, and 10.50 m respectively, than 4.50 m embedded depth for 150 kPa surcharge load. Hence, the present study took an embedded of sheet pile of 6.50 m for the entire analysis.

[Insert Fig. 5]

5.3. Influence of Footing Position on Wall Deflection and BM Behavior

To study the influence of the square and circular footing (an equal plan area of 6.25 m^2) on the SPW behavior; the footing is placed in different horizontal positions along the BGS (X-direction) and vertical positions along the depth of the SPW (Y-direction). The present analysis takes different footing positions along the BGS as X = 0.000, 2.250, and 4.500 m from the wall face. Similarly, the different positions along the depth of the SPW are taken as Y = 0.000, 1.125, 2.250, 3.375, and 4.500 m from the BGS. The plots of maximum wall deflection and BM with surcharge located at different depths from the BGS for varying horizontal positions of footings is shown in Figure 6a–6c and 6d–6f respectively, for a square footing. Figure 6a–6c and 6d–6f indicate that the maximum deflection and BM occur when the footing is positioned at the wall top edge (i.e., X = 0.000 m, Y = 0.000 m) and decreases gradually as the distance between the wall top edge and the footing increases along both the horizontal and vertical directions. Increasing the footing depth below the BGS reduces the maximum deflection and BM for a specific horizontal position. For example, an increase in depth of the footing below the BGS reduces 0.66, 0.55, 0.50, and 0.47 times the maximum wall deflection for footing positions Y = 1.125, 2.250, 3.375, and 4.500 m respectively, as compared to the position when the footing is positioned at the ground surface (Y = 0.000 m), for a horizontal position of footing X = 0.000 m with 150 kPa surcharge load as shown in Figure 6a. Similarly, an increase in the horizontal distance between the wall and the footing reduces 0.58 and 0.39 times the maximum wall deflection for footing positions X = 2.250 and 4.500 m respectively,

as compared to the position when the footing is positioned at the wall top edge (X = 0.000 m), for a vertical position of footing Y = 0.000 m with 150 kPa surcharge load as shown in Figure 6a–6c. Similarly, for a specific vertical footing position, the maximum deflection and BM decrease as the distance of the footing from the wall along the BGS increases. The deflection and BM increase as the surcharge load increases for footings placed in any particular horizontal and vertical positions; the observed trends agrees well with Aparna and Samadhiya (2020) analysis.

[Insert Fig. 6]

Figure 7a–7c and 7d–7f shows the plot of maximum deflection and BM with surcharge load respectively, for a circular footing positioned at different horizontal positions along the BGS and vertical positions along the depth of the wall. Figures indicate that increasing the surcharge increases the maximum deflection and BM significantly. Moreover, the maximum deflection and BM reduce substantially as the footing is placed away from the wall top edge. Figure 8a and 8b shows the deflection and BM profiles along the wall depth for various surcharge loads in square footing. Both the deflection and BM profile show an increase in deflection and BM with increased surcharge load.

[Insert Fig. 7]

[Insert Fig. 8]

When a circular footing with the same plan area is utilised instead of a square footing, the maximum wall deflection and BM are significantly reduced. Figures 6a, 7a, 6d, and 7d show that a circular footing placed at the wall top edge produces 0.72 and 0.67 times reduced amount of maximum deflection and BM respectively than a square footing for a 150 kPa surcharge. The reduction in the deflection and BM is due to the shape effect because, due to the uniformity of the displacement contours under the footing, the displacement of backfill soil

below the circular footing is less compared to a square footing of the same plan area; as a result, a smaller amount of lateral deformation of soil is observed for circular footings.

5.4. Influence of Surcharge Load on the Ground Settlement Behavior

Figure 9a and 9b illustrate vertical GS curves along the backfill surface with varying surcharge loads for a square and circular footing respectively, of equal plan area of 6.25 m^2 placed at the wall top edge. Figures indicate that a significantly higher GS is observed when the surcharge load increases for square and circular footing. The square footing, on the other hand, produces a higher GS than the circular footing. For example, a square footing has 1.13, 1.15, 1.18, 1.24, and 1.31 times higher values of maximum GS for 50, 75, 100, 125, and 150 kPa surcharge loads respectively, than circular footing because the displacement contours below the square footing were non-uniform and higher in magnitude than circular footing leading to a higher displacement of backfill soil below the footing.

[Insert Fig. 9]

The settlement profiles for square and circular footing indicate that a significant variation of GS is observed upto a distance of 9 m from the wall for all surcharge loads; after that distance, the variation in GS is negligible and reaches its minimum value. As a result, for all surcharge loads, the settlement influence zone acts at a distance of 2H, as illustrated in Figure 9a and 9b. The present observation agrees well with the observation of Peck (1969). Hence, reducing the risk of higher GS foundation can be located outside that zone is recommended. The normalized vertical deflection ($\delta_{v\text{-}max}$/H) under a square and circular footing has been obtained in the present study for a 100 kPa surcharge placed at the wall top edge is 0.90 and 0.76 % respectively, where $\delta_{v\text{-}max}$ is the maximum vertical GS of the backfill. Peck (1969) recommended that the normalized vertical displacement should not be more than 1.0 % in the case of flexible supports in sands. Therefore, the findings of this study are consistent

with the results recommended by Peck (1969). $\delta_{v\text{-}max}/\delta_{h\text{-}max}$ ratio is obtained as 0.64 and 0.67 for a square and circular footing respectively, with 100 kPa surcharge load, where $\delta_{h\text{-}max}$ is the maximum lateral wall deflection.

5.5. Influence of the Loose Soil Layer on the Behavior of Wall and Backfill Soils

The influence of a loose soil layer has been determined by replacing the dense soil from BGS with loose soil in layers. The depth of the loose layer (L) from the BGS is taken as 0.000, 1.125, 2.250, 3.375, 4.500, 5.625, 6.750, and 11.000 m. In the present study, the effect of a loose layer has been investigated for square and circular footing under a 125 kPa surcharge positioned at the wall top edge. Figures 10 and 11 show that wall deflection, BM, and GS profiles under square and circular footing increase significantly under a 125 kPa surcharge with increasing loose layer depth. The increment is too high when the depth of the loose layer extends below the dredge level. For example, a square footing produces 1.64 and 3.54 times higher wall deflection for loose layer depths (L) of 4.500 m (at the dredge level) and 11.000 m respectively, in comparison to the absence of a loose layer (L = 0.000 m) for a 125 kPa surcharge, as shown in Figure 10a. Similar incremental trend of results were obtained for BM and GS, as illustrated in Figure 10b and 10c respectively. The reason behind it is the decrease in the passive restraint from the frontfill soil due to the inclusion of a loose layer below the dredge level, leading to decreases in the overall stability of the CSPW. Moreover, the effect of a loose soil layer is comparatively less for circular footing. For example, a circular footing produces 0.74, 0.72, 0.62, and 0.58 times reduced wall deflections; 0.59, 0.58, 0.56, and 0.55 times lesser BMs; and 0.79, 0.73, 0.71, and 0.69 times lesser GS for loose layer depths (L) of 2.250, 4.500, 6.750, and 11.000 m respectively under 125 kPa surcharge, than square footing.

[Insert Fig. 10]

[Insert Fig. 11]

5.6. Influence of Dredge Line Slope Angle on the Sheet Pile and Ground Settlement Behavior

Dredge line inclination angles of 0º, 10º, 20º, 25º, and 30º are used to investigate how sloping dredge levels effect sheet pile and backfill GS behavior. The profiles of the wall deflection, BM, and backfill GS profiles, for a 50 kPa square footing load imposed at the wall top edge with different slope angles are displayed in Figures 12a, 12b, and 12c respectively. The results indicate a significant increase in deflection, BM, and GS with the increase in slope angles. For example, a 50 kPa surcharge load for a 10º, 20º, 25º, and 30º slope angle creates 1.30, 1.97, 3.17, and 4.67 times respectively, higher maximum deflection; 1.25, 1.62, 1.97, and 2.42 times respectively, higher maximum BM; and 1.22, 1.74, 2.30, and 3.06 times respectively, higher maximum GS, than the horizontal dredge level condition. Furthermore, Figure 12b shows that increasing the slope angle reduces the passive restraint of the wall, resulting in a decrease in the degree of fixity of the wall below the dredge level. As a result, a downward drop in the maximum BM below the dredge level is seen, with more depression recorded at greater slope angles.

[Insert Fig. 12]

6. Conclusions

In the current study, a numerical analysis with realistic 3D modeling using the FE approach was undertaken to evaluate sheet pile behavior, emphasising the shape effect of footings. Circular and square footings are placed at different locations above and below the BGS with different surcharge magnitudes to determine the sheet pile behavior. Furthermore, the effects of loose soil layers and the sloping dredge lines on the behavior of SPW are also investigated. The points to be highlighted from the present FE study are as follows:

- The deflection and BM of the sheet pile increase with the increase in the plan area of the square and circular footing. Because, a higher footing area displaces a higher amount of backfill soil below it, producing higher lateral pressure to the wall, leading to a higher wall deflection and BM. However, due to the corner effect of square footing, the displacement contours below the square footing are non-uniform and higher in magnitude than circular footing of the same plan area, leading to a higher displacement of backfill soil below the square footing, producing higher lateral pressure to the wall, leading to a higher wall deflection and BM.
- The shallow embedded depth of the wall highly influences the wall deflection and BM, due to the full mobilization of passive earth resistance (occurs upto plastic zone below the dredge level), which takes place at a larger depth for shallow embedded depth wall below the dredge level. But at the higher embedded depths the maximum deflection and BM significantly reduces because of the development of a plastic zone below the dredge level and net EP at the base of the wall decreases. This decrease in the extension of the plastic zone below the dredge level and the net EP at the base of the wall can be attributed to a significant decrease in the horizontal wall movement.
- The wall deflection and BM are maximum when the footing is positioned at the wall top edge. Increasing the distance of the footing along the BGS and along the depth of the wall from the wall top edge significantly reduces the deflection and BM. There is a significant decrease in maximum deflection and BM is witnessed when the circular footing having the same plan area is used instead of square footing due to the shape effect because, due to the uniformity of the deformation contours below the footing, the displacement of backfill soil below the circular footing is less compared to a square footing of the same plan area; as a result, a smaller amount of lateral deformation of soil is observed for circular footings.

- An increase in surcharge loads significantly increases the GS for square and circular footing. The square footing produces greater GS than the circular footing. The settlement profiles for square and circular footing show a significant variation of GS upto a distance of 2H from the wall for all surcharge loads; after that, the variation in GS is negligible and reaches its minimum value. Hence, to reduce the risk of excessive GS, it is recommended that the foundation may be placed beyond the zone of influence.
- Increasing the loose layer depth significantly increases the wall deflection, BM, and GS for square and circular footing under surcharge loads. The increment is too high when the depth of the loose layer extends below the dredge level. The reason behind it is the decrease in the passive restraint from the frontfill soil due to the inclusion of a loose layer below the dredge level, leading to decreases in the overall stability of the CSPW. Moreover, the influence of a loose soil layer is comparatively less for circular footing.
- With increasing slope angles, there is a significant increase in wall deflection, BM, and backfill GS. Increasing the dredge line slope angle reduces the wall's passive restraint, decreasing its degree of fixity below the dredge level. As a result, there is a downward drop in the point of maximum BM, with higher depression reported at steeper slope angles.

7. Acknowledgment

The authors would like to thank the National Institute of Technology Agartala for providing the laboratory facilities required to complete the research work.

8. References

ABAQUS. (2012). "Abaqus Manual [Computer Software]", Providence, RI: SIMULIA.

Ahmadpour, B., Sakhi, M.A. and Kamalian, M. (2018). "Study of Loose Soil Layer Effects on Excavations Supported by Steel Sheet Pile Walls-A Numerical Study", *Journal of Engineering Geology*, 12, 31-54. https://doi.org/10.18869/acadpub.jeg.12.5.31

Aparna. and Samadhiya, N.K. (2020). "Evaluation of model sheet pile wall adjacent to a strip footing–an experimental investigation", *International Journal of Geotechnical Engineering*, 14(7), 828-835. https://doi.org/10.1080/19386362.2019.1581459

Bahrami, M., Khodakarami, M.I. and Haddad, A. (2018). "3D numerical investigation of the effect of wall penetration depth on excavations behavior in sand", *Computers and Geotechnics*, 98, 82-92. https://doi.org/10.1016/j.compgeo.2018.02.009

Basha, A. and Elsiragy, M. (2019). "Effect of sheet pile driving on geotechnical behavior of adjacent building in sand: Numerical study", *Civil Engineering Journal*, 5(8), 1726-1737. http://dx.doi.org/10.28991/cej-2019-03091366

Bilgin, Ö. (2012). "Lateral Earth Pressure Coefficients for Anchored Sheet Pile Walls", *International Journal of Geomechanics*, 12(5), 584-595. https://doi.org/10.1061/(asce)gm.1943-5622.0000154

Bose, S.K. and Som, N.N. (1998). "Parametric study of a braced cut by finite element method", *Computers and Geotechnics*, 22(2), 91–107. https://doi.org/10.1016/S0266-352X(97)00033-5

Chowdhury, S.S., Deb, K. and Sengupta, A. (2013). "Estimation of Design Parameters for Braced Excavation: Numerical Study", *International Journal of Geomechanics*, 13(3), 234-247. https://doi.org/10.1061/(asce)gm.1943-5622.0000207

Deb, P. and Pal, S.K. (2019). "Numerical analysis of piled raft foundation under combined vertical and lateral loading", *Ocean Engineering*, 190, 106431. https://doi.org/10.1016/j.oceaneng.2019.106431

Debnath, A. and Pal, S.K. (2023a). "A numerical analysis on anchored sheet pile wall subjected to surcharge strip loading", *Journal of Engineering Research*, 11(3), 62-74. https://doi.org/10.1016/j.jer.2023.100088

Debnath, A. and Pal, S.K. (2023b). "Influence of surcharge strip loads on the behavior of cantilever sheet pile walls: A numerical study", *Journal of Engineering Research*, 11(1), 100029. https://doi.org/10.1016/j.jer.2023.100029

Design Manual. (1984). "Steel Sheet Piling United States", Steel Updated and reprinted by US Department of Transportation/FHWA with Permission.

Fall, M., Gao, Z. and Ndiaye, B.C. (2019). "Three-dimensional response of double anchored sheet pile walls subjected to excavation and construction sequence", *Heliyon*, 5(3). https://doi.org/10.1016/j.heliyon.2019.e01348

Georgiadis, M. and Anagnostopoulos, C. (1998). "Lateral Pressure on Sheet Pile Walls due to Strip Load", *Journal of Geotechnical and Geoenvironmental Engineering*, 124(1), 95-98. https://doi.org/10.1061/(asce)1090-0241(1998)124:1(95)

Guo, P., Gong, X. and Wang, Y. (2019). "Displacement and force analyses of braced structure of deep excavation considering unsymmetrical surcharge effect", *Computers and Geotechnics*, 113, 103102. https://doi.org/10.1016/j.compgeo.2019.103102

Hakeem, B. M. (2024). "Investigation Of A Loaded Pile Responses Due To Proposed Deep Excavation In Sand Soil: Finite Element Analysis using PLAXIS 3D Program", *Civil Engineering Infrastructures Journal*. https://doi.org/10.22059/CEIJ.2024.365637.1963

Hsiung, B.C.B. (2009). "A case study on the behaviour of a deep excavation in sand", *Computers and Geotechnics*, 36(4), 665-675. https://doi.org/10.1016/j.compgeo.2008.10.003

Jaky, J. (1944). "The coefficient of earth pressure at rest." *Journal of the Society of Hungarian Architects and Engineers*, 78(22), 355-358.

Li, Y., Zhang, W. and Zhang, R. (2022). "Numerical investigation on performance of braced excavation considering soil stress-induced anisotropy", *Acta Geotechnica*, 17(2), 563-575. https://doi.org/10.1007/s11440-021-01171-3

Ozpolat, A. and Aksoy, H.S. (2022). "The Effect of Distance between Sheet Pile and Foundation on Bearing Capacity of Foundation", *Advances in Civil Engineering*, 1-11. https://doi.org/10.1155/2022/7338718

Peck, R.B. (1969). "Deep excavations and tunneling in soft ground", *Proceedings of the Seventh ICSMFE, State of the Art*, pp. 225-290.

Pradeep, T., GuhaRay, A., Bardhan, A., Samui, P., Kumar, S. and Armaghani, D.J. (2022). "Reliability and prediction of embedment depth of sheet pile walls using hybrid ANN with optimization techniques", *Arabian Journal for Science and Engineering*, 47(10), 12853-12871. https://doi.org/10.1007/s13369-022-06607-w

Wang, J., Xiang, H. and Yan, J. (2019). "Numerical simulation of steel sheet pile support structures in foundation pit excavation", *International Journal of Geomechanics*, 19(4), 05019002. https://doi.org/10.1061/(ASCE)GM.1943-5622.0001373

Schroeder, W.L. and Roumillac, P. (1983). "Anchored bulkheads with sloping dredge lines", *Journal of Geotechnical Engineering*, 109(6), 845-851. https://doi.org/10.1061/(ASCE)0733-9410(1983)109:6(845)

Shafiqul Islam, M., Rokonuzzaman, M. and Sakai, T. (2017). "Shape Effect of Square and Circular Footing under Vertical Loading: Experimental and Numerical Studies", *International Journal of Geomechanics*, 17(9), 1-9. https://doi.org/10.1061/(ASCE)GM.1943-5622.0000965

Singh, A.P. and Chatterjee, K. (2020a). "Lateral earth pressure and bending moment on sheet pile walls due to uniform surcharge", *Geomechanics and Engineering*, 23(1), 71-83. https://doi.org/10.12989/gae.2020.23.1.071

Singh, A.P. and Chatterjee, K. (2020b). "Ground Settlement and Deflection Response of Cantilever Sheet Pile Wall Subjected to Surcharge Loading", *Indian Geotechnical Journal*, 50(4), 540-549. https://doi.org/10.1007/s40098-019-00387-1

Singh, A.P. and Chatterjee, K. (2020c). "Influence of soil type on static response of cantilever sheet pile walls under surcharge loading: a numerical study", *Arabian Journal for Geosciences*, 13. https://doi.org/10.1007/s12517-020-5170-x

Sowers, G.B. and Sowers, G.F. (1967). "Failures of bulkhead and excavation bracing", *Civil Engineering*, 37(1), 72-77.

Tabaroei, A., Sarfarazi, V., Pouraminian, M. and Mohammadzadeh, D. (2022). "Evaluation of behavior of a deep excavation by three-dimensional numerical modeling", *Periodica Polytechnica Civil Engineering*, 66(3), 967-977. https://doi.org/10.3311/PPci.20353

Tsinker, G.P. (1983). "Anchored Sheet Pile Bulkheads: Design Practice", *Journal of Geotechnical Engineering*, 109(8), 1021-1038.

Wood, D.M. (2004). "Geotechnical modelling (Applied Geotechnics; V. 1)", Boca Raton FL USA, CRC Press Taylor & Francis Group/Books.

Zhang, R., Goh, A.T.C., Li, Y., Hong, L. and Zhang, W. (2021). "Assessment of apparent earth pressure for braced excavations in anisotropic clay", *Acta Geotechnica*, 16, 1615-1626. https://doi.org/10.1007/s11440-020-01129-x

TABLES

Table 1. Description of soil [after Singh and Chatterjee (2020a, 2020c)]

Type of soil	Properties			
	Unit weight [γ] (kN/m^3)	Friction angle [φ] (degree)	Poisson's ratio [μ]	Young's modulus [E] (MPa)
Dense sand	18.40	39	0.30	90
Loose sand	14.00	30	0.38	36

Table 2. Description of SPW [after USS Manual (1984) and Bilgin (2012)]

Section provided	Cross-sectional area (cm^2/m)	Elastic section modulus (cm^3/m)	Moment of inertia (cm^4/m)
PZ27	168.10	1620	25200

Table 3. Specifications of the model SPW and footing

Parameters	Symbols	Scaling laws	Numerical model (Prototype)	Experimental model
SPW material	−	1	Steel	Steel
Height of sheet pile above the dredge level (cm)	H	1/n	450	15
Depth of embedment (cm)	D	1/n	650	21.67
Cross-sectional area (cm^2/m)	A_p	$1/n^2$	168.10	0.19
Moment of inertia (cm^4/m)	I	$1/n^4$	25200	31.11×10^{-3}
Young's modulus of the pile (GPa)	E	1	200	200
Plan area of footing (cm^2)	A_F	$1/n^2$	62500	69.44
Thickness of the footing plate (cm)	t	1/n	40	1.33

Table 4. Parameters used for the parametric study

Parameters	Symbol	Values

The magnitude of the surcharge load (kPa)	q	50, 75, 100, 125, and 150
Plan area of square and circular footing (m^2)	A	1.00, 2.25, 4.00, 6.25, 9.00, and 12.25
Embedded depth of wall (m)	D	4.50, 6.50, 8.50 and 10.50
Position of square and circular footing from the wall face along the BGS (m)	X	0.000, 2.250, and 4.500
Position of square and circular footing from the BGS along the depth of wall (m)	Y	0.000, 1.125, 2.250, 3.375, and 4.500
Depth of loose soil layer (m)	L	0.000, 1.125, 2.250, 3.375, 4.500, 5.625, 6.750, and 11.000
Dredge line slope angle (º)	α	0, 10, 20, 25, and 30

FIGURES

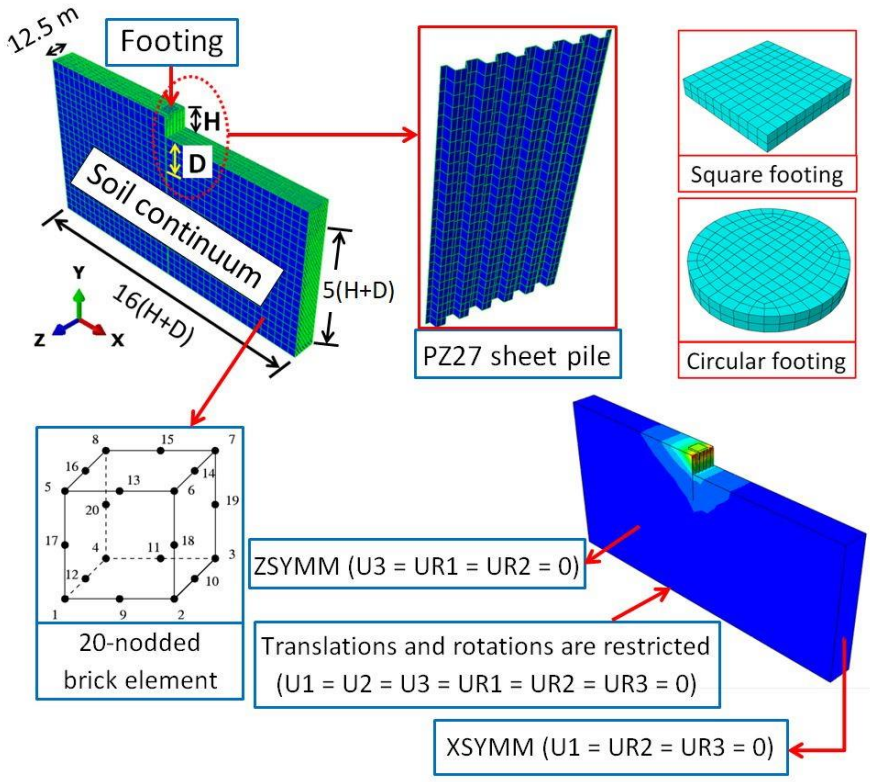

Fig. 1. Dimensions, element type, model meshing and model boundaries adopted for the numerical study

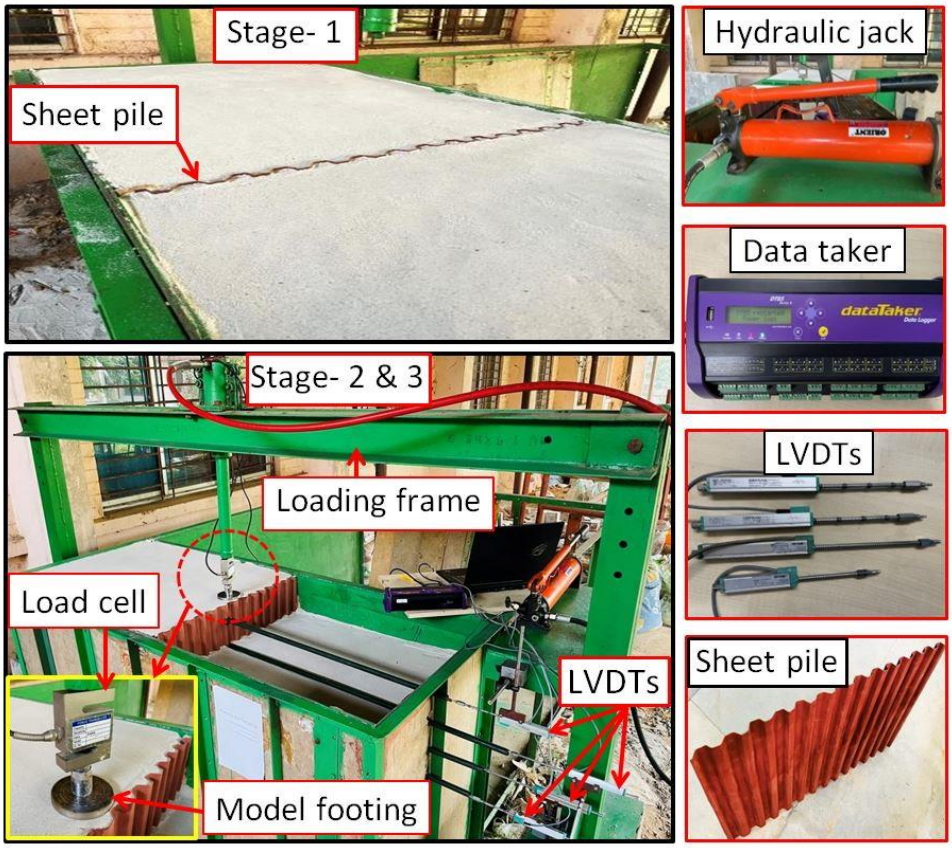

Fig. 2. Experimental test set-up

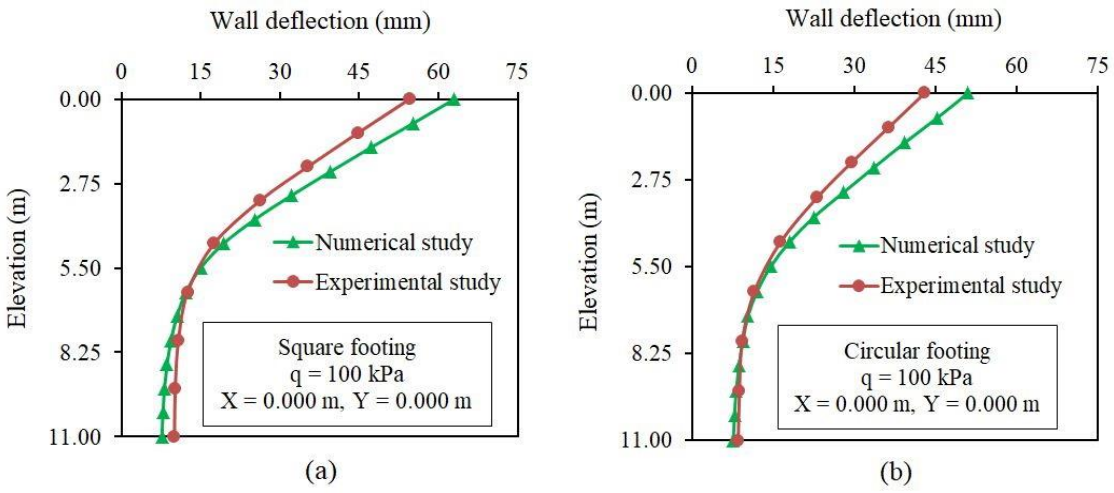

Fig. 3. Wall deflections obtained in the present numerical and experimental studies for: (a) square footing; and (b) circular footing

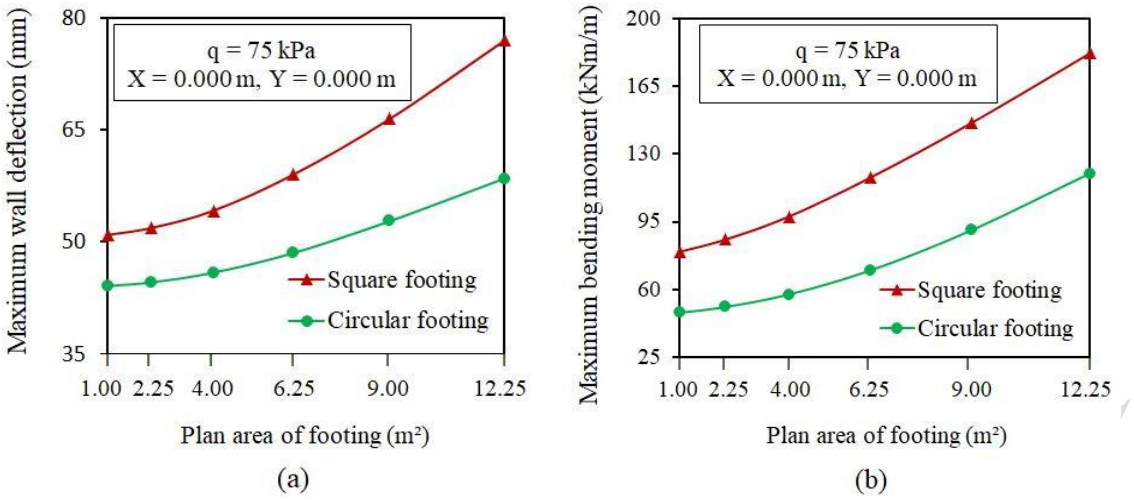

Fig. 4. Effect of varying plan area of square and circular footing for dense sand on maximum: (a) wall deflection; and (b) BM

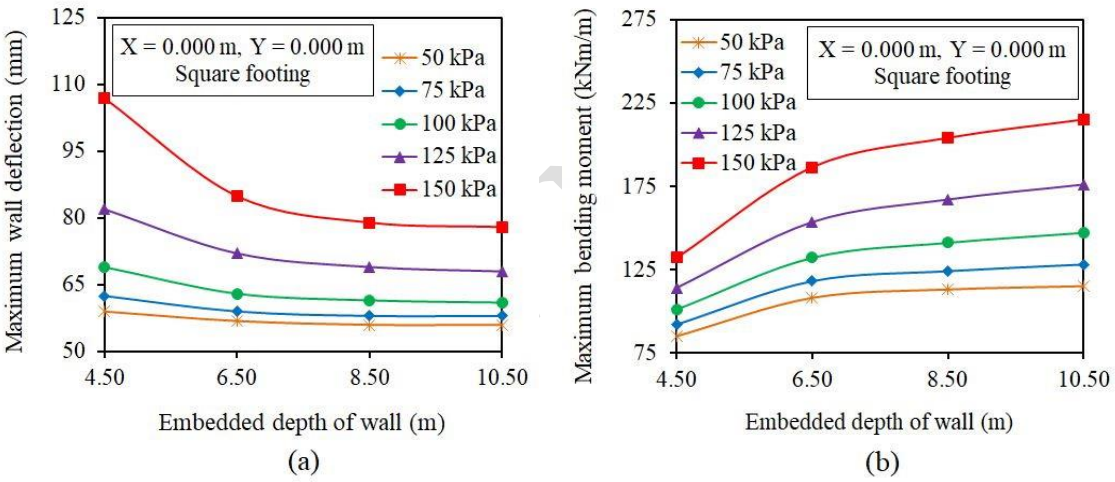

Fig. 5. Effect of varying embedded depths with square footing on maximum: (a) wall deflection; and (b) BM

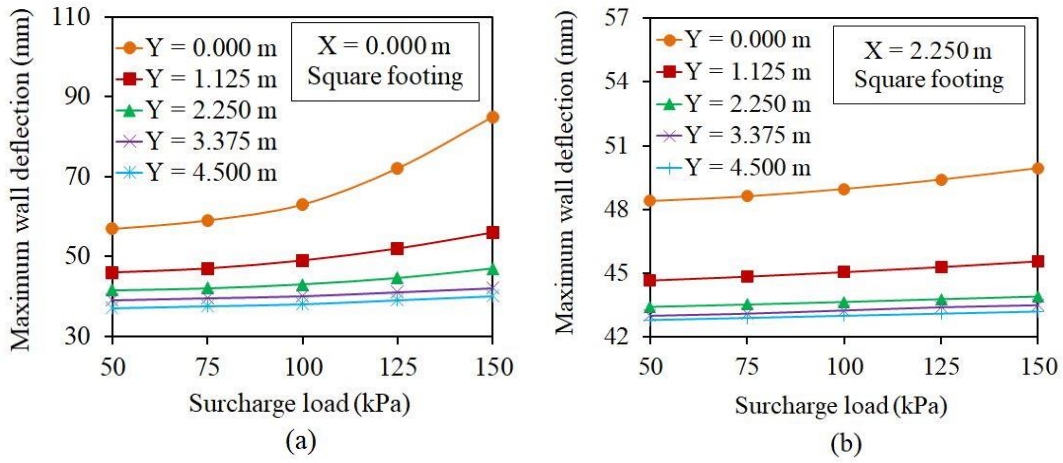

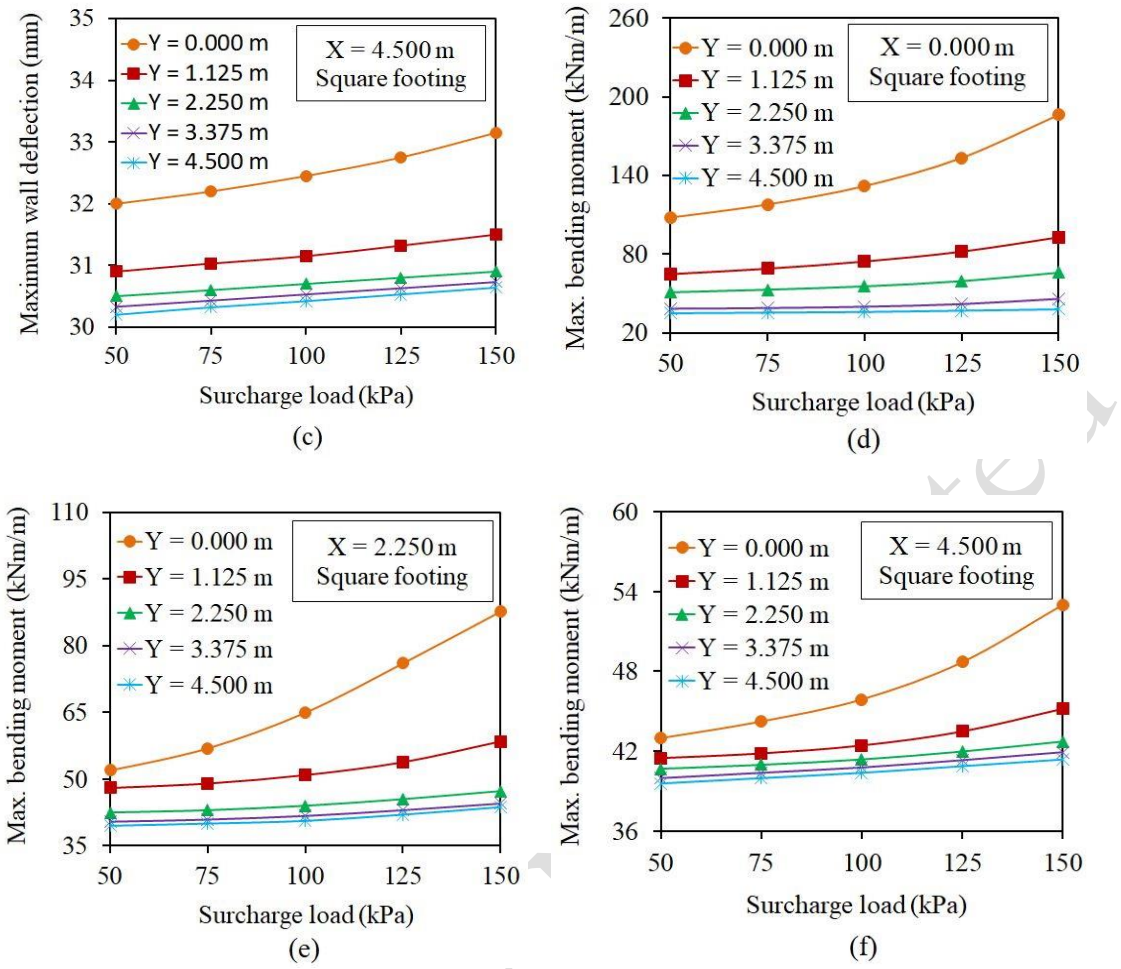

Fig. 6. Plot of maximum: (a–c) wall deflection; and (d–f) BM under the surcharge load for a square footing with locations varying vertically and horizontally

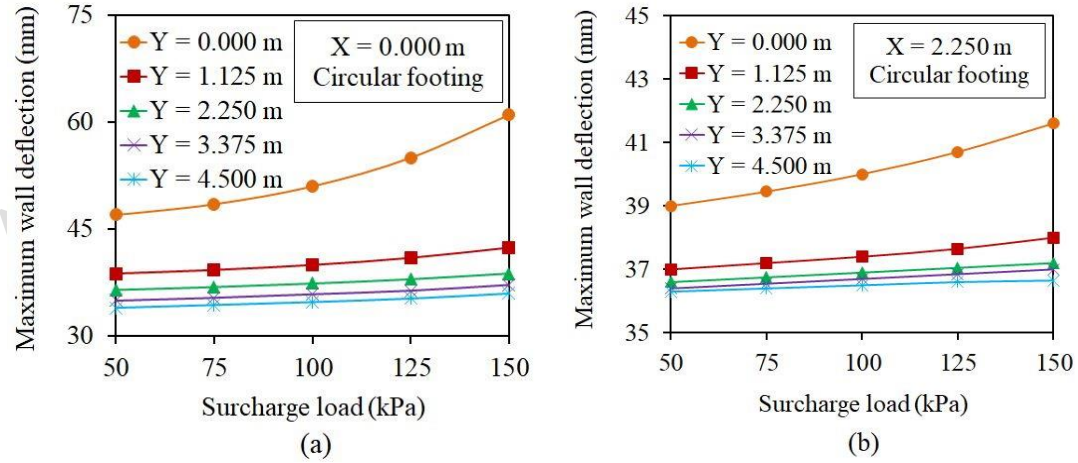

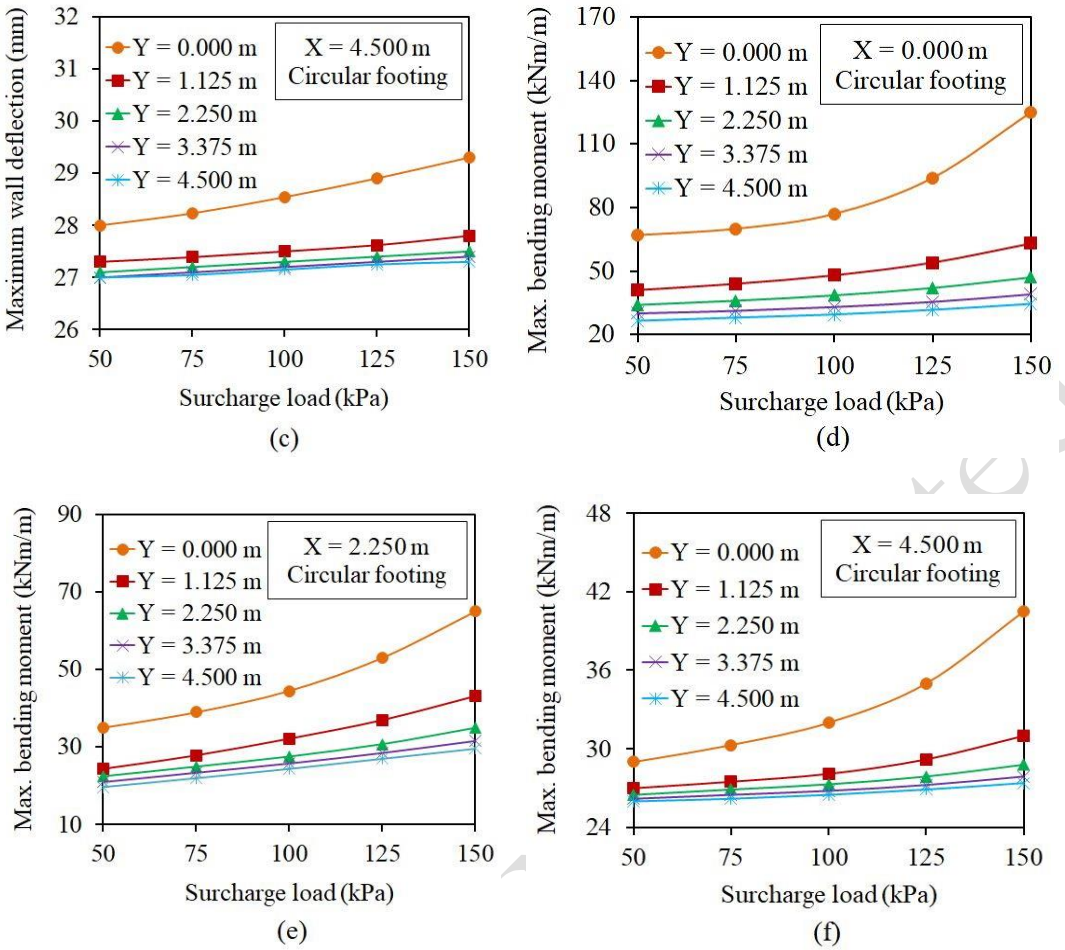

Fig. 7. Plot of maximum: (a–c) wall deflection; and (d–f) BM under the surcharge load for a circular footing with locations varying vertically and horizontally

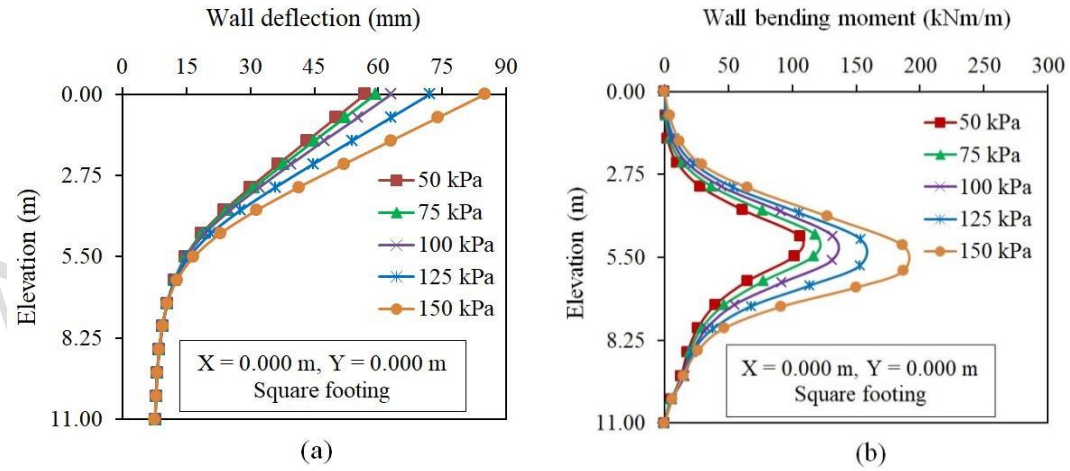

Fig. 8. (a) Wall deflection; and (b) BM profiles with different surcharge loads for square footing placed at the wall top edge for dense sand

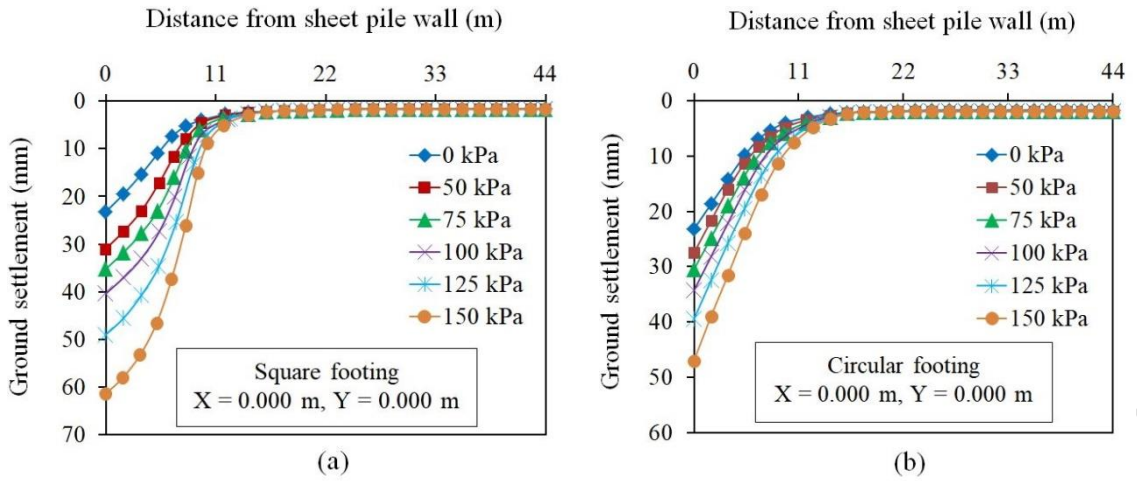

Fig. 9. Variation of vertical GS along the BGS under various surcharge loads placed at the wall top edge (X = 0.000 m, Y = 0.000 m) for: (a) square footing; and (b) circular footing

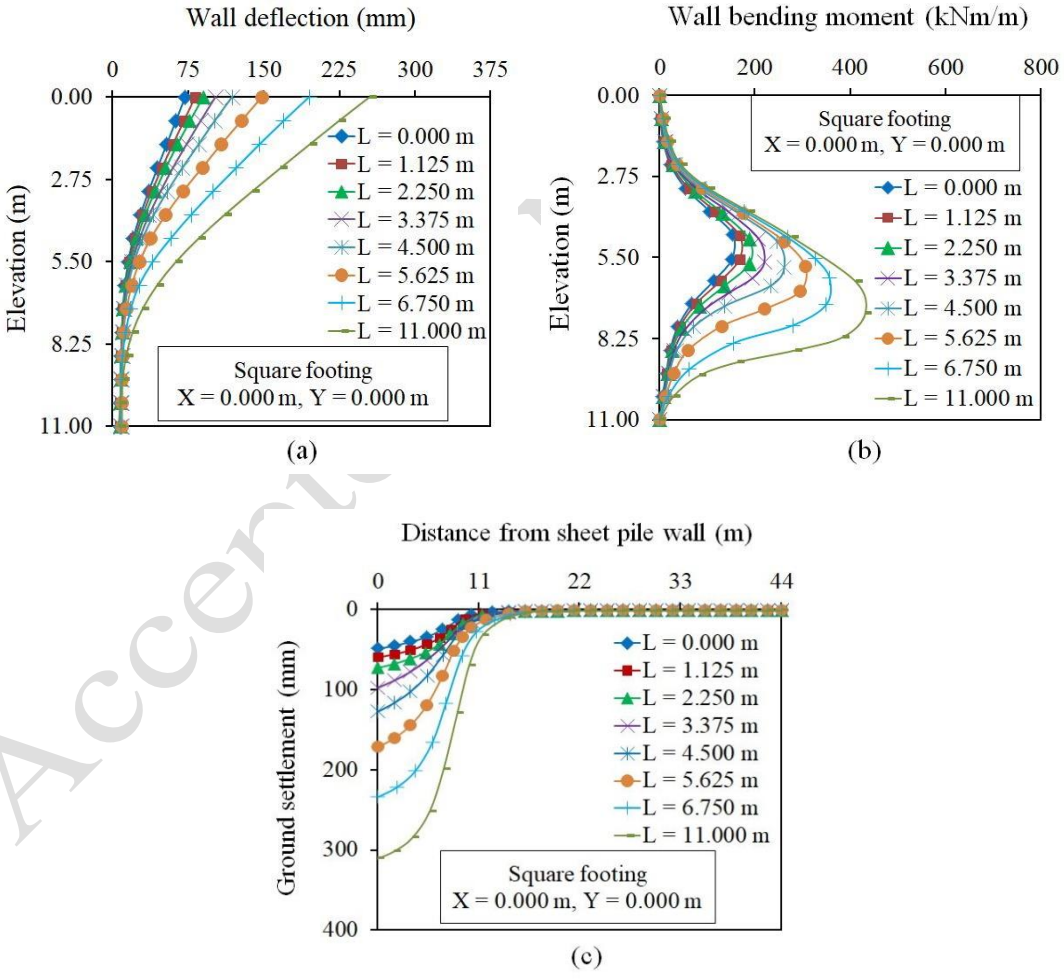

Fig. 10. Plot of (a) wall deflection; (b) BM; and (c) GS, for a square footing with 125 kPa surcharge load placed at the wall top edge

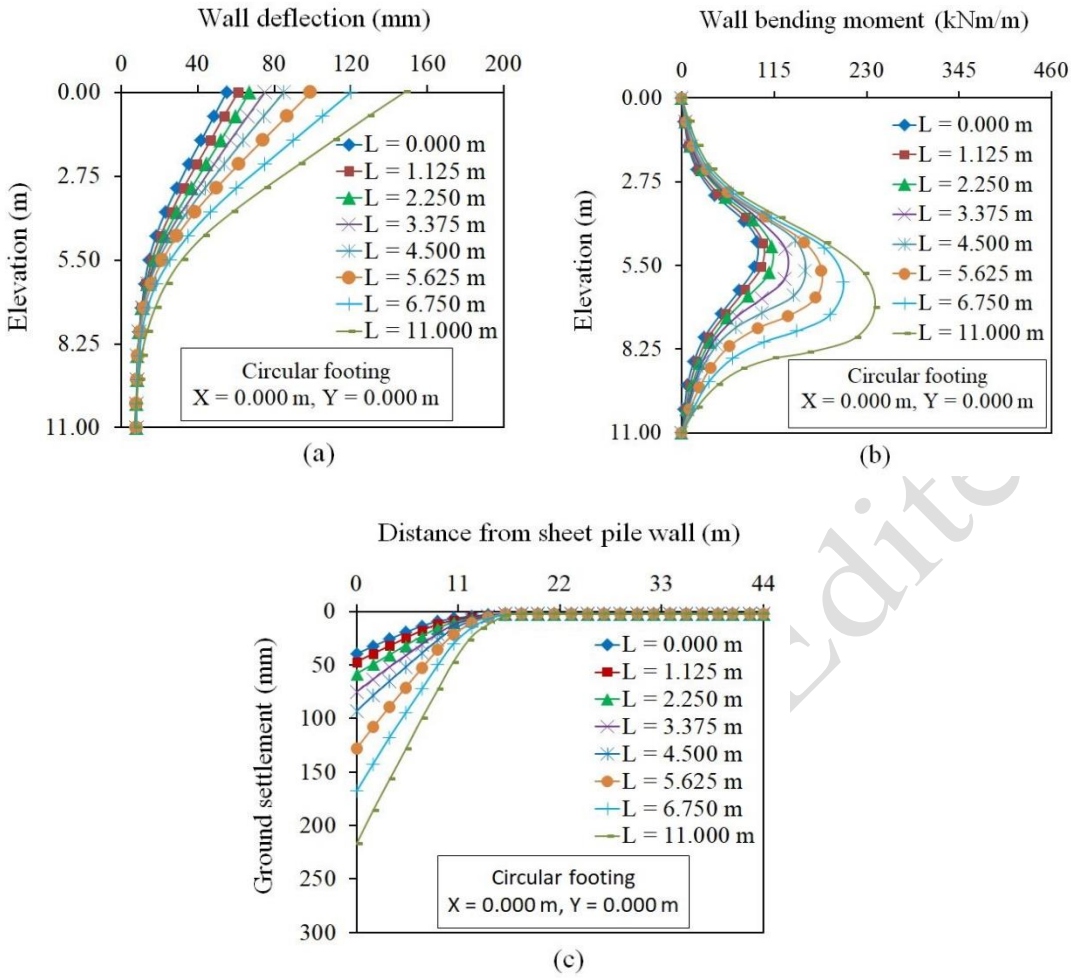

Fig. 11. Plot of (a) wall deflection; (b) BM; and (c) GS, for a circular footing with 125 kPa surcharge load placed at the wall top edge

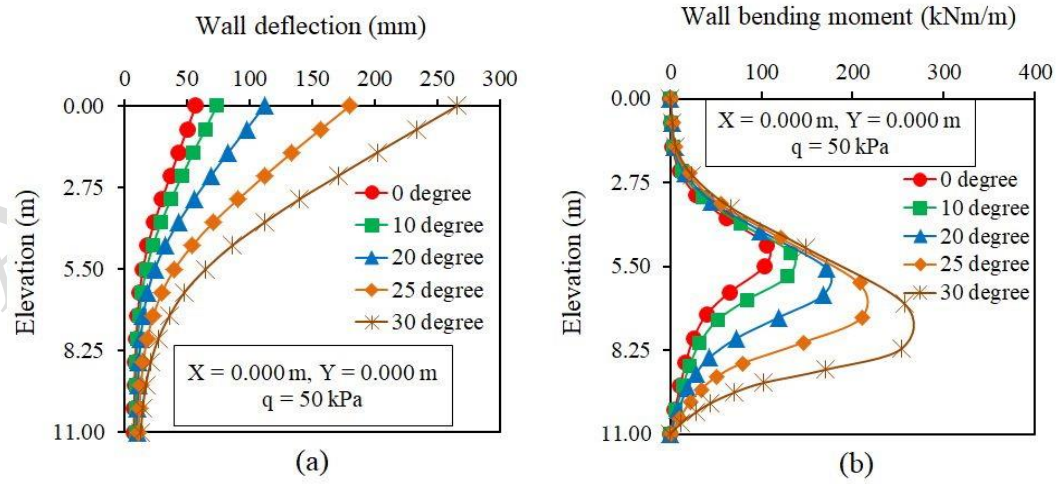

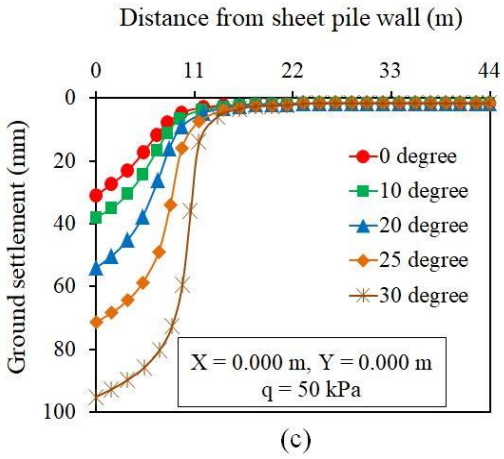

Fig. 12. Plot of (a) wall deflection; (b) BM; and (c) GS, for a square footing with 50 kPa surcharge load placed at the wall top edge for various dredge line slope angles